Proceeding of the IEEE
International Conference on Robotics and Biomimetics
Dali, China, December 2019

Design and Modeling of a 2-DOF Cable-Driven Parallel Wrist Mechanism

Hao Jiang, Cai Xiao, Jian Li, Yu Zhong, Tao Zhang*, and Yisheng Guan*
Biomimetic and Intelligent Robotics Lab (BIRL)
School of Electro-mechanical Engineering
Guangdong University of Technology
Guangzhou, Guangdong Province, China, 510006

***Abstract*—This paper proposes a novel design of 2-DOF Cable-Driven Parallel Wrist Mechanism (CDPWM). This mechanism can achieve hemispherical movement in space which has a unconventional twin actuation. The configuration has a great flexibility (with no singular points within the entire motion range), and a large stiffness of 1.07×10^6 Nmm/rad. This work utilized a vector analysis method to establish the kinematic model of this construction and the stiffness performance of the mechanism was also analyzed. The proposed model can deeply simplify the kinematics solution of this type of cable driven system with a maximum position error of 0.03 mm. Based on this method, the velocity Jacobian of the mechanism was also constructed. Then the stiffness of the mechanism was theoretically modeled, and validated through the finite element method (FEM).**

***Index Terms*—Parallel Mechanism; Kinematics; Stiffness Analysis;**

I. INTRODUCTION

With the improvement of industrial automation and development of science and technology, such as artificial intelligence, robotics has brought a big change to the whole world. This change enables human production methods to move from handicraft, mechanization and automation to the era of intelligence [1]. Robot has always been an important field for scholars in various countries, and as an important part of humanoid robots, robotic wrists attract numerous scientists and engineers' attention.

Many novel designs of robot arm wrists have been proposed in industrial and academic fields, but there is no wrist could carry a relatively high payload yet having excellent flexibility. For example, conventional robot wrists (such as iiwa of KUKA, the universal robot (UR)) [2] used for industrial robots are simple and safe, however, their weight is heavy, and producing singular points under some specific poses. Parallel mechanisms can reduce the size and weight, yet these mechanisms usually have a complex configuration, and are difficult in gaining a simple kinematic relationship between actuators and tip positions. The well-known wrist mechanism, Omni-Wrist III [3], can realize circular rolling, but it is impossible for cable actuation due to its link interference and drive mode. For the LIMS1 wrist [4], who can implement a spherical rolling motion with a bevel mechanism and wire coupling is complex and heavy.

In general, two drivers are essential to make a wrist mechanism produce a 2-DOF movement. However, owning to the property that flexible cables can only be pulled rather than be pushed, almost all previous designs utilized three actuations [5, 6] apart from some flexible link. The elephant trunk [7] use two actuations to keep the length of cables constant, however, a pulley compensating system is added making the system bulky. The other twin actuation is the robot (CDSLRA) [8] which uses a soft backbone, however, this design can only maintain the tension of one pair cable, which diminish the configuration' stiffness.

In addition, significant efforts in cable-driven robot have been done on the kinematics of parallel wrist [9, 10]. However, there is still not a simple and straightforward approach, which can achieve real-time control. Moreover, there is also scant information about stiffness analysis of cable-driven wrists, all the current situation leads to inadequate carrying capacity evaluation of wrist arms.

In this paper, a parallel wrist mechanism is designed to achieve hemisphere movement while having a unique twin actuation. Through incorporating anti-parallelogram theory into the CDPWM, the cables can be kept tight under any situation. Next, kinematics of this system is proposed, and according to kinematic model, the Jacobian matrix of this CDPWM is calculated. Finally, a stiffness analysis method is illustrated and validated for the cable driven system.

II. BASIC CONCEPT OF CDPWM : CURRENT AND PROPOSED DESIGNS

Most robot wrists using for facial manipulators are 3 degree of freedom, which is consistent to human arm. A wide motion range of a delicate mechanism to reduce singular poses are extremely important to wrists, due to their important influence on operational performance of a manipulator. However, designing a light-weight and high-load wrist mechanism to overcome all the aforementioned issues are very difficult. Many robot wrists have been demonstrated in academic, such as CDSLRA robot [11]. In general, they posses backbones, rigid universal

* Corresponding authors, tzhang@gdut.edu.cn, ysguan@gdut.edu.cn. The work in this paper is partially supported by the Natural Science Foundation of China (Grant No. 51905105), the Natural Science Foundation of Guangdong (Grant No. 2015A030308011), and the Frontier and Key Technology Innovation Special Funds of Guangdong (Grant No. 2016B090911002,2017B090910008, 2017B090910002). and the Guangdong Yangfan Program for Innovative and Entrepreneurial Teams (Grant No. 2017YT05G026).

978-1-7281-6321-5/19//$31.00 ©2019 IEEE

or spherical joints, disks and cables. On the basis of backbone design, robot wrists can be divided into two types: one employ rigid backbone which are connected by universal/spherical joints [12], while the other applies a flexible backbone[13] which is made of elastic material.

A. Properties of existing wrist robots

1) Flexibility and stiffness: They are very important property index determining mechanism's performance. For wrist mechanisms with rigid backbone, the flexibility of which depends on its configurations' bending angle, and the bending angle is determined and limited by the universal/spherical joints' range, their flexibility will perform poor due to the limited universal range. For wrist mechanism with flexible backbone, the mechanism can generate a great bending angle which demonstrate the flexibility is excellent. However, this configuration is sparing in backbone's stiffness, which severely restrict the payload capability.

2) Actuation: There are two common ways: one employs three independent pairs cables/actuators to drive parallel mechanism, and the other utilizes two pairs actuators/cables. Most of the existing wrist mechanisms are using the former due to its simplicity in control. The latter actuation method can minimize the mechanism's weight and size, however, the flexible backbone and the rigid backbone cannot directly apply the dual drive method, owing to the tension problem caused by cables length (Fig. 1) discussed below.

Fig. 1(a) show cable tension challenge using flexible backbone of robot wrist. Let L and L' be the length of flexible backbone and removing between points A and B, respectively, and l_{left} , l_{right} and l'_{left}, l'_{right} be the cable lengths in initial state and after-actuation state, respectively. we can easily get the geometrical equation from the initial state

$$l_{left} + l_{right} = 2L = 2L' \tag{1}$$

From the after-actuation configuration of Fig. 1(a), we can obtain

$$l'_{left} + l'_{right} = 2L' < 2L \tag{2}$$

According to Eqs. 1 and 2, we can easily get

$$l'_{left} + l'_{right} < l_{left} + l_{right} \tag{3}$$

According to Eq. 3, the length of cable will change with the mechanism's movement and cannot keep constant, so driving cables cannot be stretched tight when the wrist is moving. Similar to wrist with flexible backbone, the wrist robot using rigid backbone shown in Fig. 1(b) occur the same issue either. Therefore, the flexible backbone and the rigid backbone cannot directly apply twin actuation/cables without any tension compensating system.

B. New conception for wrist configuration

For overcoming the challenge of flexibility or stiffness, a novel wrist structure is proposed, who can solve aforementioned issues and apply two actuations method.

The design philosophy is that anti-parallelogram can produce pure rolling along two ellipses, and by extending this rule to 3-dimensional space, a new parallel mechanism approximating 2 DOF elliptical movement is put forward (Fig. 4). Fig. 2(a) shows the anti-parallelogram and its relative ellipse, which is indicated by red line. Let s_e and l_e be the short and long link, and h_e be the distance between two disks in straight pose, respectively. Then this ellipse can be denoted as

$$\frac{x^2}{(s_e/2)^2} + \frac{y^2}{(h_e/2)^2} = 1 \tag{4}$$

$$l_e^2 = s_e^2 + h_e^2 \tag{5}$$

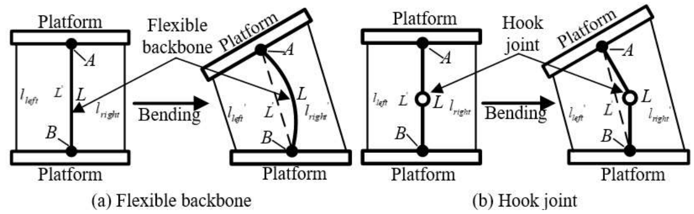

Fig. 1: Kinematic challenge for twin actuation

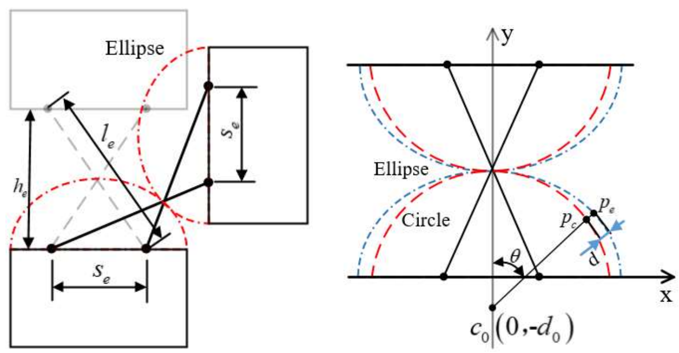

Fig. 2: (a) Anti-parallelogram generate a rolling along two ellipses; (b) Circle approximate the ellipse rolling

In order to keep cable length constant when this mechanism is moving, supposing that there exists a circle which can approximate the ellipse in motion range, the center c_0 is placed towards y coordinate with an offset d_0 from origin (Fig. 2(b)). Assuming a line from c_0 to a point on ellipse p_e while it intersects equivalent circle at p_c. Then this line and equivalent circle can be expressed as

$$x - tan\theta \cdot y - tan\theta \cdot d_0 = 0 \tag{6}$$

$$x^2 + (y + d_0)^2 = r^2 \tag{7}$$

while θ illustrates the angle between this line and y coordinate. By solving Eqs. (4) and (6), we get the position of p_e (x_e, y_e), and solving Eqs. (6) and (7), we can get the position of p_c (x_c, y_c). Let $d(\theta)$ be the deviation of p_e and p_c

$$d(\theta) = \sqrt{(x_c - x_e)^2 + (y_c - y_e)^2} \tag{8}$$

If the value $d(\theta)$ remains zero, it means this method can equivalent ellipse motion to circular rolling.

Owning to maximum length of humans wrist is near 60 mm, basing on this criterion, we set s_e, l_e and d_0 as 20, 60, and 3.05 mm, respectively. By using iterative searching method to minimize $d(\theta)$, it can reach zero within maximum error of 0.03 mm, as shown in Fig. 3. It can be validated proper geometric parameter can help anti-parallelogram accomplish circular rolling within acceptable deviation.

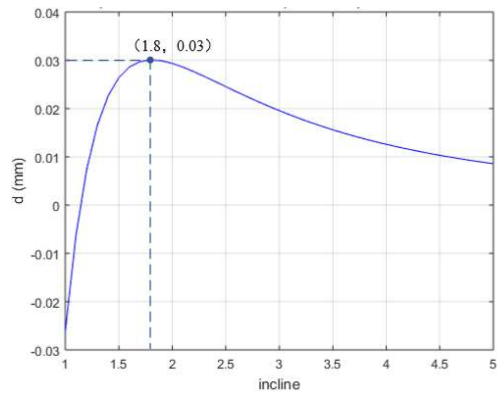

Fig. 3: Position error between ellipse and equivalent circle

III. Description of the CDPWM

The proposed mechanism (Fig. 4) consist of base plate, moving plate and linkages, the linkages are fixed between two plates to restrict their movement range. They are driven by two pairs cables, owing to intrinsic characteristic moving as circular rolling, it can avoid tension problem in motion, and its driving actuators are installed remotely to make the wrist lightweight.

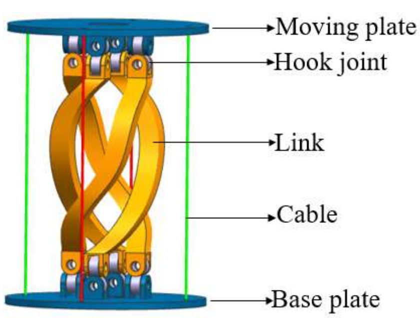

Fig. 4: The prototype of CDPWM

A. Kinematic analysis

In this section, the kinematic relationship between cable length and bending angle is discussed. By incorporating the anti-parallelogram theory into the twin actuation design, the cable in this wrist can be kept constant and tensioned well.

1) Forward kinematic: To obtain the position of CDPWM with change of cable length, the forward kinematic is modeled. In this model, the four linkages are simplified to act as a rigid backbone.

In Fig. 5(b), O_1 and O_2 are middle points of the two plates, respectively, where coordinate of O_1XYZ and O_2XYZ are attached. The angle α and β denotes the bending direction and the bending angle, respectively.

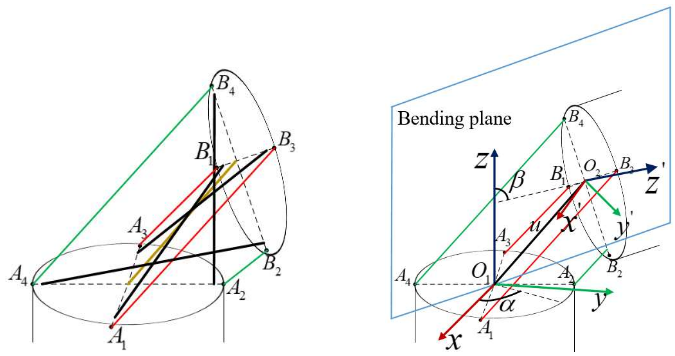

Fig. 5: (a)The CDPWM configuration, (b)The CDPWM coordinate

Due to each driving pair cables' length is constant, therefore, the kinematics can be considered to be composed of two parts/pairs. As shown in Fig. 5(a), equivalent link (the gray line) is parallel with driving cables in bending plane. Hence, the vector projection of vector O_1A_i on vector O_1O_2 is $(l_i - S)/2 (i = 1, 2)$, and the equation is

$$O_1A_i \cdot O_1O_2 = \frac{l_i - S}{2} \quad (9)$$

where S is the length of equivalent rigid backbone and l_i are the lengths of cables.

Substituting vector $O_1O_2(x_u, y_u, z_u)$ and the known vector $O_1A_i(x_i, y_i, 0)$ into Eq. (9) to produce Eq. (10)

$$x_u x_i + y_u y_i = \frac{l_i - S}{2}(i = 1, 2) \quad (10)$$

where $A_1(x_1, y_1, 0)$, $A_2(x_2, y_2, 0)$ are known through the design of mechanism.

From Eq. (10), the parameter x_u and y_u can be calculated, and $O_1O_2(x_u, y_u, z_u)$ can be obtained.

Based on the obtained vector $O_1O_2(x_u, y_u, z_u)$ (Fig. 5(b)), the bending direction and bending angle are

$$\begin{cases} \alpha = tan^{-1}(\frac{y_u}{x_u}) \\ \beta = \pi - 2tan^{-1}(\frac{z_u}{\sqrt{x_u^2+y_u^2}}) \end{cases} \quad (11)$$

2) Inverse kinematic: To obtain the cable length at a known position and orientation of CDPWM, the inverse kinematics is modeled through two steps: First, get the position of moving plates B_i by bending direction and bending angle, then, computing the magnitude of vector A_iB_i, the length of driving cable can be obtained.

As shown in Fig. 6(a), the vector of O_1B_i of each cable are

$$O_1B_i = O_1O_2 + O_2B_i \quad (12)$$

According to the intrinsic conversion relationship of this wrist, the orientation of vector O_2B_i can be obtained by rotating O_1A_i about bending angle β with regard to vector

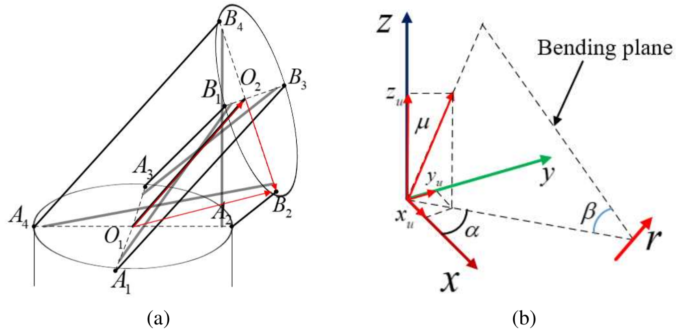

Fig. 6: (a) Kinematic model of the CDPWM, (b) Unit vector presentation,

r, who is the intersection vector between moving plate plane and base plane (Fig. 6(b)). Firstly, the vector of axis r can be expressed as

$$r = \begin{bmatrix} k_x \\ k_y \\ k_z \end{bmatrix} = \begin{bmatrix} cos(\pi/2+\beta) \\ sin(\pi/2+\beta) \\ 0 \end{bmatrix} \tag{13}$$

The rotation matrix R_T is

$$R_T = \begin{bmatrix} a_{11} & a_{12} & a_{13} \\ a_{21} & a_{22} & a_{23} \\ a_{31} & a_{32} & a_{33} \end{bmatrix} \tag{14}$$

where $a_{11} = k_x \cdot k_x \cdot vs + cs$, $a_{12} = k_y \cdot k_x \cdot vs - k_z \cdot sn$, $a_{13} = k_z \cdot k_x \cdot vs + k_y \cdot sn$, $a_{21} = k_x \cdot k_y \cdot vs + k_z \cdot sn$, $a_{22} = k_y \cdot k_y \cdot vs + cs$, $a_{23} = k_z \cdot k_y \cdot vs - k_z \cdot sn$, $a_{31} = k_x \cdot k_z \cdot vs - k_y \cdot sn$, $a_{32} = k_y \cdot k_z \cdot vs + k_x \cdot sn$, $a_{33} = k_z \cdot k_z \cdot vs + cs$, $cs = cos(\beta)$, $sn = sin(\beta)$, $vs = 1 - cs$.

According to Eqs. (13) and (14), O_2B_i can be written as

$$O_2B_i = R_T \cdot O_1A_i \tag{15}$$

As shown in Fig .6(a), the vector O_1O_2 can be expressed as

$$O_1O_2 = \begin{bmatrix} S \cdot cos(\varphi) \cdot cos(\alpha) \\ S \cdot cos(\varphi) \cdot sin(\alpha) \\ S \cdot sin(\varphi) \end{bmatrix} \tag{16}$$

where $\varphi = \beta/2$.

Substituting Eqs. (15) and (16) into Eq. (12) to produce Eq. (17)

$$O_1B_i = O_1O_2 + R_T \cdot O_1A_i \tag{17}$$

Therefore, the vector A_iB_i can be written as

$$A_iB_i = O_1O_2 + R_T \cdot O_1A_i - O_1A_i \tag{18}$$

Hence, the length $l_i (i = 1, 2, 3, 4)$ of cable can be derived by computing the magnitude A_iB_i, then we get the inverse kinematic equation.

$$l_i = |A_iB_i| = |O_1O_2 + R_T \cdot O_1A_i - O_1A_i| \tag{19}$$

B. Stiffness analysis

Stiffness analysis of parallel mechanism at given points of workspace can be represented by stiffness matrix. This matrix demonstrates relationship of force/torque applied at moving plate between responding linear/angular displacement who can be obtained using kinematic and dynamic equations.

To control the velocity of CDPWM, we described the Jacobin matrix, which represents the relationship between angular velocity $\dot{\theta} = [\dot{\alpha}, \dot{\beta}]$ and linear velocities of the cables $V = [V_1, V_2]$

$$V = J \cdot \dot{\theta} \tag{20}$$

where V_1 and V_2 are linear velocities of each driving cables, respectively.

Differentiating Eq. (12) towards time, produce the linear velocity of point B_i

$$V_{Bi} = \begin{bmatrix} V_{xi} \\ V_{yi} \\ V_{zi} \end{bmatrix} = (J_{O_1O_2} + J_{O_2B_i}) \begin{bmatrix} \dot{\alpha}_i \\ \dot{\beta}_i \\ 0 \end{bmatrix} \tag{21}$$

where $J_(O_1O_2) + J_{O_2B_i}$ is a 3×3 Jacobin matrix for B_i.

From Fig. 6(a), we can know the linear velocity of cable is along the direction of equivalent backbone, thus dot-multiplying both sides of Eq. (21) by vector μ, we can get

$$V_i = \mu \cdot V_{Bi} = \mu \cdot (J_{O_1O_2} + J_{O_2B_i}) \cdot \begin{bmatrix} \dot{\alpha}_i \\ \dot{\beta}_i \\ 0 \end{bmatrix} \tag{22}$$

Hence, the matrix

$$J_i = \begin{bmatrix} J_{i1} & J_{i2} & J_{i3} \end{bmatrix} = \mu \cdot (J_{O_1O_2} + J_{O_2B_i}) \tag{23}$$

is a 1×3 matrix for the Jacobin of ith driving pair.

Since the third vector of angular velocities in Eq. (21) is zero, thence, the Jacobian matrix could be altered to

$$V = J_s \cdot \dot{\theta} \tag{24}$$

where

$$J_s \begin{bmatrix} J_{11} & J_{12} \\ J_{21} & J_{22} \end{bmatrix} \tag{25}$$

is a 2×2 matrix for the Jacobin of the CDPWM.

The stiffness of parallel mechanism depends on many factors, such as size and types of the linkage, actuating method, and so on. To simplify the analysis process, assuming steel cable is the main factor [14]. It can be denoted as

$$F = K\Delta X \tag{26}$$

where F is the vector of force/moment applied on moving plate, K is the stiffness matrix, ΔX mean displacement variance of moving plate. In stiffness equation, K can be written as [15]

$$K = J^T k J \tag{27}$$

where J is the Jacobin matrix of wrist and k express element stiffness with a 2×2 matrix. For proposed design of wrist, cable is the main influential factor, then K can be written as

$$K = J^T_{cable} k_{cable} J_{cable} \tag{28}$$

where $k_{cable} = \begin{bmatrix} k_1 & 0 \\ 0 & k_2 \end{bmatrix}$, $J_{cable} = \begin{bmatrix} J_1 & J_2 \end{bmatrix}$ is the structure matrix associated with the driving cables, $J_i = \begin{bmatrix} A_iB_i \\ R_T O_2 B_i \times A_iB_i \end{bmatrix} (i = 1, 2)$ is the cable vector, and A_iB_i is the directional unit vector of the ith cable.

IV. Simulation and verification

Kinematics and stiffness of the CDPWM are verified by simulation (ADAMS) in this section. Set the dimension to: $O_1A_i = 25mm$, $O_2B_i = 25mm$, and the height of two plate in vertical direction is 60 mm. For actuation method, the movement of cables are simplified as translational motion.

A. Verification of kinematics

To compare the error between theoretical model and simulation results, we set the rotation range of each actuator and get all the tip position of CDPWM (Fig. 7 is the workspace of CDPWM) by using kinematic model and simulation tool (ADAMS), the deviation curve between the theoretical model and the simulation are shown in Fig. 8.

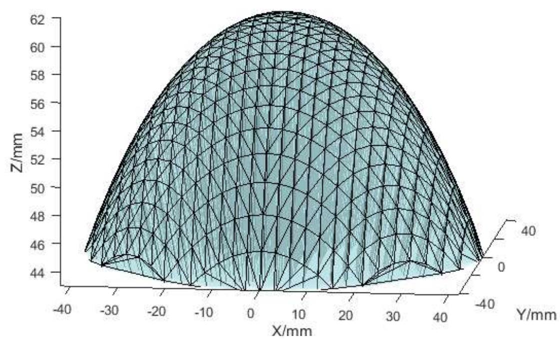

Fig. 7: The CDPWM workspace

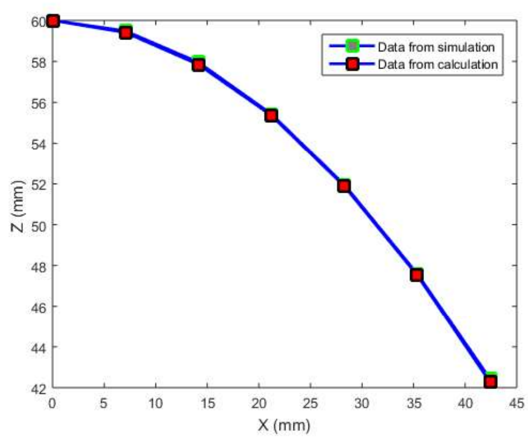

Fig. 8: Tip position comparison between calculation and simulation

Fig. 8 shown the result by kinematic model almost coincides with the curve of simulation model. The maximum position error is 0.03 mm, therefore, the kinematic model can be used to represent the CDPWM.

B. Verification of stiffness

Based on Eq. (26), the deflection of CDPWM at given position is calculated by moment applied on moving plate. Compare the FE model result with the theoretical, the stiffness property can be verified.

In this simulation model (Fig. 9), the cable is substituted by springs owing its property to produce elongation be pulled. Set the spring stiffness at $600N/mm$, equaling to stiffness of $0.75mm$ commercial steel cable, and moment applied on moving plate is $160Nmm$.

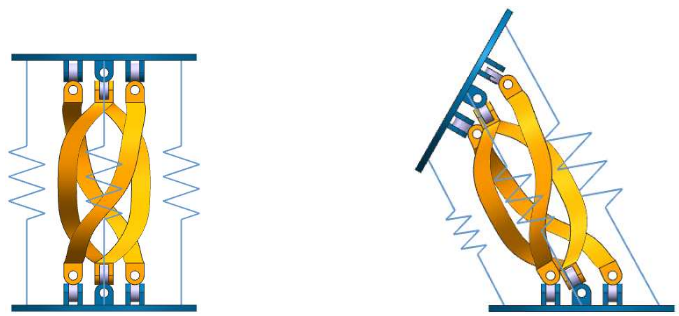

(a) Simulation($0°$) (b) Simulation($60°$)

Fig. 9: Stiffness simulation model of the CDPWM

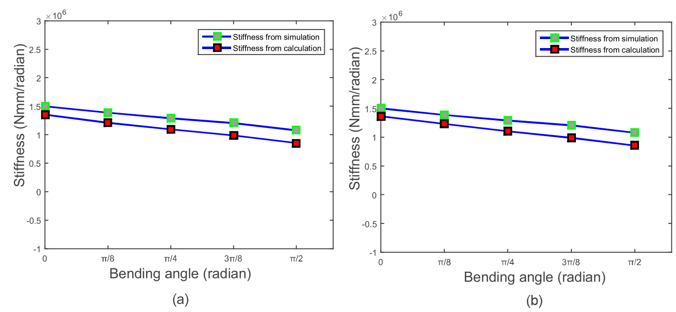

Fig. 10: (a)Stiffness at direction angle $0°$, (a)Stiffness at direction angle $60°$

The stiffness of CDPWM (at direction angle $0°$and $60°$) are got by theoretical and simulation model (Fig. 10). Regarding to bending angle, the maximum error between theoretical and simulation mode is 9%, and the deflections caused by 160 N mm end load (at direction angle $0°$ and $60°$) are presented in Fig. 11, the maximum deflection is $1.49 \times 10^{-4} rad (0.0085°)$ happening at $90°$. According to acceptable variance, the stiffness model can be used to present CDPWM.

V. Conclusion

In this paper, a unique 2-DOF wrist mechanism was proposed. The biggest difference between this design and others is employing twin actuation method to drive the wrist while having high flexibility (with no singular points through the entire hemispherical range) performance and a compact lightweight structure. Based on this design, a simple, faster to compute, kinematic model is proposed. Compared with the

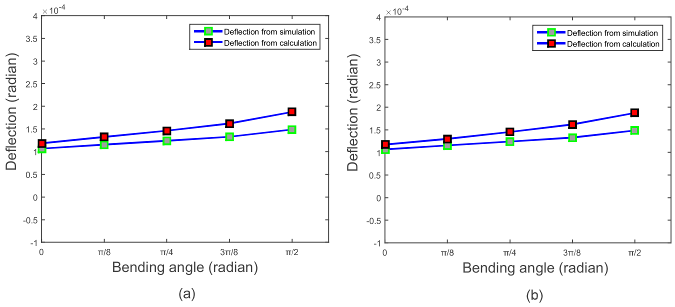

Fig. 11: (a)Deflection at direction angle 0°, (b)Deflection at direction angle 60°

simulation results, it is found that this theoretical model is very close to the simulation results with a maximum position error of 0.33 mm. On the basis of this kinematic model, Jacobian matrix is proposed to evaluate the stiffness while the maximum error between theoretical and simulation results is only 9%. Thus, the theoretical model presented in this paper can accurately and effectively describe the kinematics and stiffness of the CDPWM. In the future, the prototype of wrist will be manufactured based on the results of this study to analyze its performance experimentally.

References

[1] D. J. Williams, H. I. Krebs, and N. Hogan, "A robot for wrist rehabilitation," in *2001 Conference Proceedings of the 23rd Annual International Conference of the IEEE Engineering in Medicine and Biology Society*, vol. 2. IEEE, 2001, pp. 1336–1339.

[2] R. Bischoff, J. Kurth, G. Schreiber, R. Koeppe, A. Albu-Schäffer, A. Beyer, O. Eiberger, S. Haddadin, A. Stemmer, G. Grunwald *et al.*, "The kuka-dlr lightweight robot arm-a new reference platform for robotics research and manufacturing," in *ISR 2010 (41st International Symposium on Robotics) and ROBOTIK 2010 (6th German Conference on Robotics)*. VDE, 2010, pp. 1–8.

[3] M. E. Rosheim and G. F. Sauter, "New high-angulation omnidirectional sensor mount," in *Free-Space Laser Communication and Laser Imaging II*, vol. 4821. International Society for Optics and Photonics, 2002, pp. 163–175.

[4] Y.-J. Kim, "Anthropomorphic low-inertia high-stiffness manipulator for high-speed safe interaction," *IEEE Transactions on Robotics*, vol. 33, no. 6, pp. 1358–1374, 2017.

[5] I. D. Walker and M. W. Hannan, "A novel'elephant's trunk'robot," in *1999 IEEE/ASME International Conference on Advanced Intelligent Mechatronics (Cat. No. 99TH8399)*. IEEE, 1999, pp. 410–415.

[6] M. B. Pritts and C. D. Rahn, "Design of an artificial muscle continuum robot," in *IEEE International Conference on Robotics and Automation, 2004. Proceedings. ICRA'04. 2004*, vol. 5. IEEE, 2004, pp. 4742–4746.

[7] M. Hannan and I. Walker, "The'elephant trunk'manipulator, design and implementation," in *2001 IEEE/ASME International Conference on Advanced Intelligent Mechatronics. Proceedings (Cat. No. 01TH8556)*, vol. 1. IEEE, 2001, pp. 14–19.

[8] Z. Zhang, G. Yang, S. H. Yeo, W. B. Lim, and S. K. Mustafa, "Design optimization of a cable-driven two-dof joint module with a flexible backbone," in *2010 IEEE/ASME International Conference on Advanced Intelligent Mechatronics*. IEEE, 2010, pp. 385–390.

[9] K. Xu and N. Simaan, "Analytic formulation for kinematics, statics, and shape restoration of multibackbone continuum robots via elliptic integrals," *Journal of Mechanisms and Robotics*, vol. 2, no. 1, p. 011006, 2010.

[10] G. Lum, S. Mustafa, H. Lim, W. Lim, G. Yang, and S. Yeo, "Design and motion control of a cable-driven dexterous robotic arm," in *2010 IEEE Conference on Sustainable Utilization and Development in Engineering and Technology*. IEEE, 2010, pp. 106–111.

[11] Z. Zhang, "Design optimization of a cable-driven two-dof flexible joint module," *International Journal of Advanced Robotic Systems*, vol. 9, no. 5, p. 213, 2012.

[12] C. B. Yigit and P. Boyraz, "Design and modelling of a cable-driven parallel-series hybrid variable stiffness joint mechanism for robotics," *Mechanical Sciences*, vol. 8, no. 1, pp. 65–77, 2017.

[13] K. Xu and N. Simaan, "Actuation compensation for flexible surgical snake-like robots with redundant remote actuation," in *Proceedings 2006 IEEE International Conference on Robotics and Automation, 2006. ICRA 2006.* IEEE, 2006, pp. 4148–4154.

[14] C. Gosselin, "Stiffness mapping for parallel manipulators," *IEEE Transactions on Robotics and Automation*, vol. 6, no. 3, pp. 377–382, 1990.

[15] D. Chakarov, "Study of the passive compliance of parallel manipulators," *Mechanism and Machine Theory*, vol. 34, no. 3, pp. 373–389, 1999.